Experiments on Contact Charging for an Electrostatic Microparticle Thruster

IEPC-2009-010

Presented at the 31st International Electric Propulsion Conference,
University of Michigan • Ann Arbor, Michigan • USA
September 20 – 24, 2009

Thomas Trottenberg*, Viktor Schneider† and Holger Kersten‡
IEAP, Christian-Albrechts-Universität zu Kiel, D-24118 Kiel, Germany

Abstract: This paper reports on first experiments aiming at an efficient technique for contact charging of microparticles, which could be applied for space propulsion. Fine electrode structures create high electric field strengths at the particle surface when a conductive microparticle comes in contact with the high voltage electrode. Besides propulsion of space vehicles, terrestrial applications for surface treatment and as a new particle source for hypervelocity experiments like simulation of micrometeorites appear possible.

Nomenclature

C	= capacitance
d_1, d_2	= width and separation of conductive lines
D_i	= surface charge density at the particle surface element i
E_i	= electric field strength at the particle surface element i
E_p	= electric field strength at the particle surface
e	= elementary charge
ϵ_0	= permittivity of free space
F	= electrical field force acting on a charged microparticle
P_acc	= acceleration power
ϕ_p	= surface potential of a particle
m_p	= particle mass
$\dot{N}_\mathrm{p}$	= particle ejection rate
q_p	= particle charge
r_n	= radius of curvature of a needle tip
r_p	= particle radius
R	= resistance
ρ	= mass density of a microparticle
T	= thrust
U_HV	= high voltage potential
ΔU	= amplitude of the particle detector signal
v_p0	= velocity of a particle after acceleration

*Research Associate, Plasma Technology, trottenberg@physik.uni-kiel.de
†Research Associate, Plasma Technology, schneider@physik.uni-kiel.de
‡Professor, Plasma Technology, kersten@physik.uni-kiel.de

I. Introduction

TODAY ELECTROSTATIC propulsion is still a synonym for ion thrusters. However, the idea of using particles even heavier than ions with high atomic mass numbers, i.e. molecules, clusters, nano- and microparticles, suggests itself and is not new.[1,2] The expected advantage of heavy particles over simply increasing the ion current in a conventional ion thruster is due to the fact, that electrostatic ion engines suffer from the space-charge limitation of the ion current (Child-Langmuir law), so that higher currents would require larger grid areas. The thrust

$$T = (2P_{\mathrm{acc}} m_{\mathrm{p}} \dot{N}_{\mathrm{p}})^{\frac{1}{2}} \tag{1}$$

can be written as a function of the available power for acceleration P_{acc}, the mass of an accelerated particle m_{p} and the particle ejection rate $\dot{N}_{\mathrm{p}}$. This shows that "ions" with higher mass would also result in an increased thrust. In the end it is the mass flow rate, i.e. the product of particle mass and ejection rate, which determines the thrust, since the acceleration power can be considered as a constant.

Concepts for heavy particle thrusters are still in the stage of preliminary experiments and proposals. The most developed concept is based on field emission thrusters which are operated in the ion-droplet mixed regime (colloid thrusters).[3] Promising, though still unrealized, are nanoparticle thrusters which extract charged particles from a suspension by means of electric fields. The functional principle has already been shown in a scaled-up experiment with spherical and needle-shaped particles of sizes from more than a millimeter down to a few tens of micrometers.[4]

In this contribution, we propose contact charging of solid metal or conductively coated dielectric microparticles and their electrostatic acceleration as a novel thruster concept. The principle has been used for almost five decades in experiments for the simulation of micrometeorites,[5,6] but is, as implemented there, not efficient enough for an application as thruster. The aim of our investigations is the improvement of this technique with regard to a reliable and high particle charging and a high mass flow rate. We report on preliminary experiments with electrode assemblies of different geometries and the particle diagnostic for charge and speed of the charged microparticles. The preparation of the next step, which is the fabrication of miniaturized electrodes in MEMS technology, is described.

II. Contact Charging

A. Starting Point: Hypervelocity Experiments

Hypervelocity experiments for the simulation of micrometeorites and their impacts for example on the surface of the moon, space vehicles, space suits and instruments also use electrostatic acceleration of charged microparticles. A successful technique applied there allows charging close to the physical limits (see below). The particles are brought in contact with very small spherical or needle-shaped surfaces at high voltage potentials, as indicated in Fig. 1(a). Shelton et al.[5] applied this technique using as charging electrode a tapered tungsten wire with a diameter of $2r_{\mathrm{n}} = 24\ \mu$m at the tip, which is maintained at a positive potential of $U_{\mathrm{HV}} = +20$ kV. When a microparticle ($r_{\mathrm{p}} < r_{\mathrm{n}}$) touches the needle tip, it acquires the charge

$$q_{\mathrm{p}} = \frac{2}{3}\pi^3 \epsilon_0 r_{\mathrm{n}} \frac{r_{\mathrm{p}}^2}{(r_{\mathrm{p}} + r_{\mathrm{n}})^2} U_{\mathrm{HV}} \quad , \tag{2}$$

when the needle tip is assumed to be a small sphere. With the assumption $r_{\mathrm{n}} \gg r_{\mathrm{p}}$, the electric field strength on the particle becomes $E_{\mathrm{p}} = \pi^2 U_{\mathrm{HV}}/6r_{\mathrm{n}}$ after separation from the electrode. For example a needle tip with radius $r_{\mathrm{n}} = 12\ \mu$m at a potential of $U_{\mathrm{HV}} = +20$ kV yields an electric field strength of $E_{\mathrm{p}} = 2.7 \times 10^9\ \mathrm{V m^{-1}}$. A 1 μm iron particle ($\rho = 7874\ \mathrm{kg\,m^{-3}}$) would carry 475 000 positive elementary charges and have a specific charge of $q_{\mathrm{p}}/m_{\mathrm{p}} = +18.5\ \mathrm{C\,kg^{-1}}$. The values for a ten times smaller 100 nm particle are $q_{\mathrm{p}} = +4750e$ and $q_{\mathrm{p}}/m_{\mathrm{p}} = +185\ \mathrm{C\,kg^{-1}}$. Of course, a singly-charged xenon ion has a much higher specific charge ($7.3 \times 10^5\ \mathrm{C\,kg^{-1}}$).

Dielectric particles can also be charged with this technique, but they have to be coated with a conducting material. In the Heidelberg Dust Accelerator coated latex particles were successfully used.[7]

B. Improvements

The charging technique applied in the previously mentioned hypervelocity experiments has two disadvantages with respect to a thruster application. First, the charging process is not well reproducible, often particles do

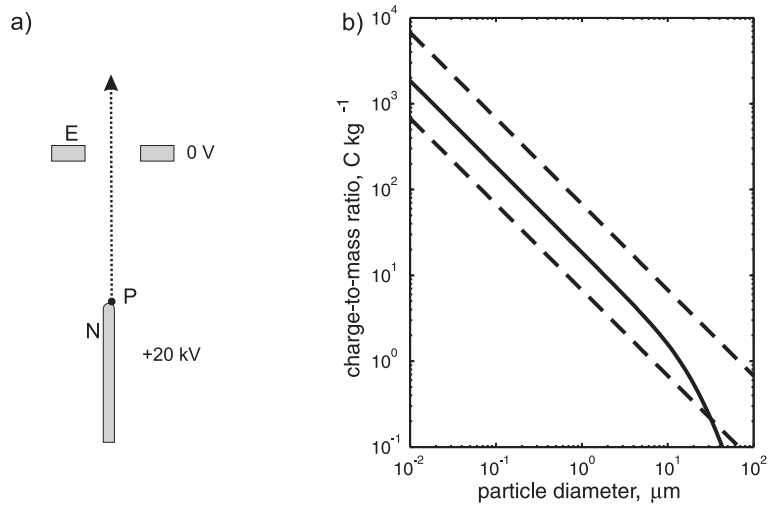

Figure 1. (a) Schematic of particle charging and acceleration. The particle P is charged at the needle N, is accelerated towards the electrode E, and leaves the system through the hole in the electrode. (b) Expected specific charge for spherical iron particles (24 μm needle tip at $\pm$20 kV). Dashed lines show the limitation due to electron field emission (lower line) and field evaporation (upper line).

not reach the desired charge. This can be explained with particles which are charged at the lateral surface of the needle where the electric field strength is much less than at the tip, and consequently, the particles are charged much less. In those experiments a suitable solution is to sort out particles of the "wrong" charge using a particle selection unit.[7] But in case of a microparticle thruster this would be a waste of propellant and energy. Second, a particle source with a single high voltage electrode does not yield sufficiently high mass flow rates.

We applied two ideas in order to overcome these disadvantages. The first one is to embed laterally the needle in a dielectric. This ensures, that the microparticles can touch the electrode only at the tip where the field strength is highest. The second idea is the use of many small electrode surfaces ("needle tips") integrated in a planar dielectric surface in order to allow many simultaneous charging processes.

C. Upper Limits for the Particle Charge

The electric charge on a microparticle is limited by two processes which become important at very high electric field strength on the particle surface.[8] For negative charges electron field emission begins at $|E_\mathrm{p}| > 10^9$ $\mathrm{V\,m^{-1}}$. For positive charges field evaporation destroys the particle, if $|E_\mathrm{p}| > 10^{10}$ $\mathrm{V\,m^{-1}}$. In case of materials with low tensile strength or fluffy grains, charges of both signs are able to fragment the particles ("Coulomb explosion")[9] already at lower field strengths.

The specific charge $q_\mathrm{p}/m_\mathrm{p}$, which is the crucial parameter for electrostatic acceleration, can be related to the electric field at the surface $E_\mathrm{p} = q_\mathrm{p} \,/\, 4\pi\epsilon_0 r_\mathrm{p}^2$, assuming spherical particles. By means of the particle mass $m_\mathrm{p} = \frac{4}{3}\pi r_\mathrm{p}^3 \rho$, one obtains the specific charge as

$$\frac{q_\mathrm{p}}{m_\mathrm{p}} = 3\frac{\epsilon_0 E_\mathrm{p}}{r_\mathrm{p}\rho} \quad . \tag{3}$$

This equation can be used to calculate the maximum possible specific charge, which depends on the particle size and density and the critical electric field strengths for positive and negative charges.

Figure 1(b) shows the expected charge-to-mass ratios for the contact-charging technique. In case of spherical iron particles charged by contact with a 20 kV needle, electron field emission would limit negative charging, meanwhile positively charged particles are not yet affected by field evaporation. For this reason only positive charging potentials should be applied.

III. Experiments

A. Preliminary Experiments

Prior to the microfabrication of electrodes, we performed some experiments with truncated metal wires and foils embedded in epoxy resin. Figure 2 shows the fabrication steps of such a dielectrically embedded electrode. A circuit board with the back contact is screwed together with lateral mold pieces. An aluminum foil (12.5 μm) or gold wires (diam. 25 μm) are connected to the back contact and clamped between the back contact and a temporary plate screwed on top of the mold pieces. Now, epoxy resin of very low viscosity is poured into the cavity. After hardening, the plate and the mold pieces are removed and the surface is made even with a milling machine and polished. The cutting edge of the foil or the wires, which is now flush with the dielectric surface, forms the electrode surface.

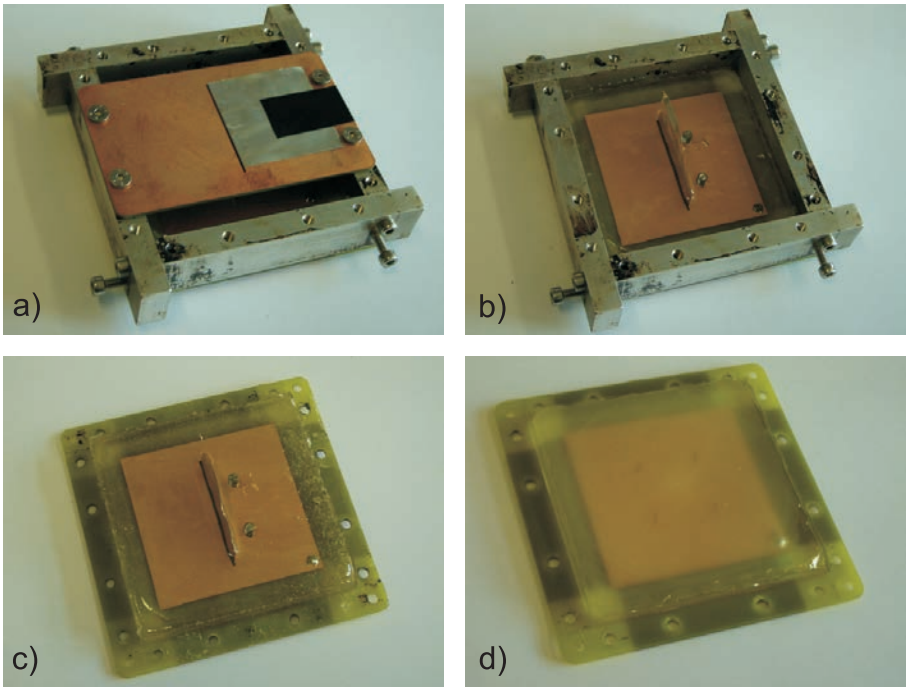

Figure 2. Resin casting of embedded electrodes. (a) Mold with a clamped aluminum foil, (b) mold after filling with liquid epoxy resin and hardening, (c) the electrode after removing of the mold. (d) Electrode array after milling and polishing of the surface (an array of fine gold wires and four stronger copper wires instead of a metal foil are used in this photograph).

As counter electrode serves a grounded metal plate with holes or slits (for wire or foil electrodes, respectively) a few millimeters above the electrode surface. Both are mounted in a vacuum chamber (see Fig. 3) and the high-voltage electrode is connected via its back contact to a 20 kV voltage source. The vacuum chamber is pumped down to a pressure below 10^{-4} Pa.

The microparticles can be injected in vacuum from top through the opening in the counter electrode (not applied so far) or the electrode surface is coated before assembly with a thin layer of particles. For this purpose, the surface is covered with a suspension of 3 μm gold-coated microspheres in isopropanol. The alcohol evaporates within a few seconds and the particles remain firmly on the surface due to adhesive forces. After pumping down, the high voltage is switched on. Immediately and during a very short time, many particles are ejected through the opening in the grounded electrode.

Figure 4 shows the electrode surface after such a "shot". On the photo the vicinity up to 2 mm around the electrode became free from particles after application of the high voltage. This can be explained by the strong electric field in the vicinity of the electrode inducing a dipole in the conductive particle, which in turn feels the dipole force in direction of the gradient of the field, i.e. toward the electrode. At longer distances this force is not sufficient to overcome the adhesive force, which explains that the more distant particles remained on the surface. The ejected particles can be collected with a glue strip above the opening in the grounded electrode, but a more sophisticated diagnostic is described in the following subsection.

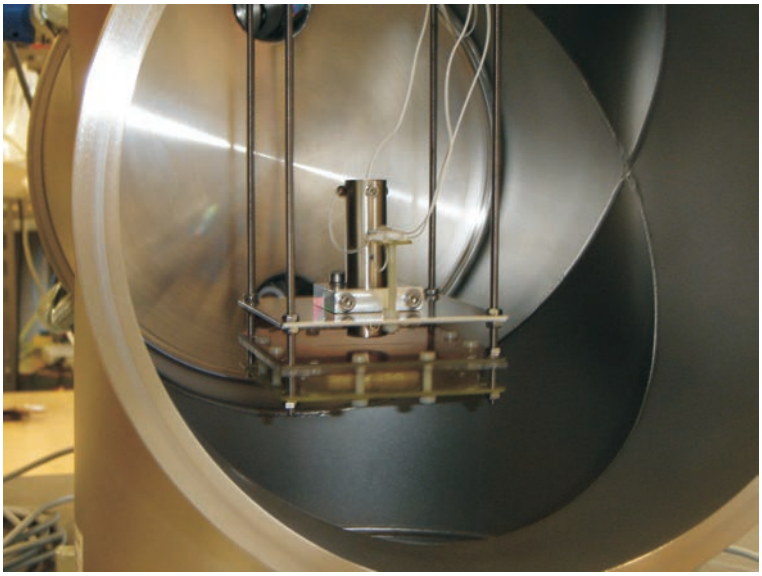

Figure 3. View into the vacuum chamber. Four thread rods hold the particle source, i.e. the embedded electrode and the counter electrode. The aluminum plate with the vertical cylinder above the particle source is the particle detector with impedance converter.

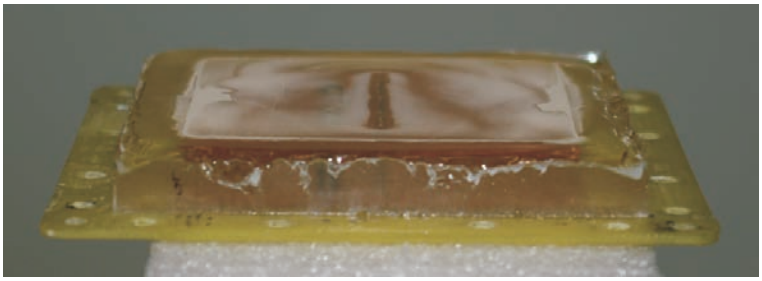

Figure 4. Electrode, which was prepared with a particle coating, after being connected to high voltage. Particles in the vicinity of the electrode were attracted, charged and accelerated.

B. Particle Detection

The particle detector follows the example of the detectors used in devices for the simulation of micrometeorites, which make use of electrostatic induction.[5,7,10] A sketch of the detector is shown in Fig. 5. When a particle with charge q_p flies through the inner one of two cylinders, which form a capacitor, it induces the same charge q_p on the outside of the inner cylinder, and the corresponding voltage over the capacitor can be measured. The voltage signal is trapezoid-like with steep edges, which allows a time-of-flight measurement of the particle speed. The signals have to be measured with very high input impedance and must not to be altered by stray capacitances of the measuring circuit. Therefore, a FET operational amplifier positioned as close as possible to the detector cylinders serves as an impedance converter, so that the amplified signals can be measured with a conventional digital oscilloscope.

A resistor $R = 50$ GΩ parallel to the detector removes charges which stem from particles grazing the inner cylinder. The resistor R together with the detector capacitance C yield a damping time constant $\tau = RC$. A measurement of this constant, which is approximately half a second, allows an accurate determination of the effective detector capacitance $C \approx 10$ pF. The knowledge of the detector capacitance is important for the calculation of the particle charge q_p. It is

$$q_\mathrm{p} = C\Delta U \qquad , \tag{4}$$

where ΔU is the amplitude of the voltage signal produced at the detector.

Although our first experiments with the epoxy resin electrodes were able to charge and accelerate particles,

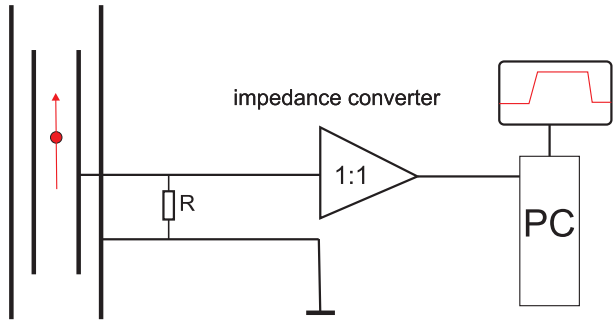

Figure 5. Particle detector with impedance converter.

the diagnostic of particle charge and speed with the particle detector was not possible so far. The reason is, that too many particles left the source at the same time and grazed the detector, which overcharged the detector electronic. To overcome this problem, we currently work on a particle dispenser which drops single particles onto the electrode.

C. Miniaturization

Microelectromechanical systems (MEMS) technology allows not only a more compacted, but also a much preciser fabrication of embedded electrodes than our epoxy resin technique described above. We are currently producing small chips (2×2 cm^2) with thin gold lines on a glass wafer. The gaps between the lines are silicon dioxide. Figure 6 shows schematic side and top views of an electrode chip.

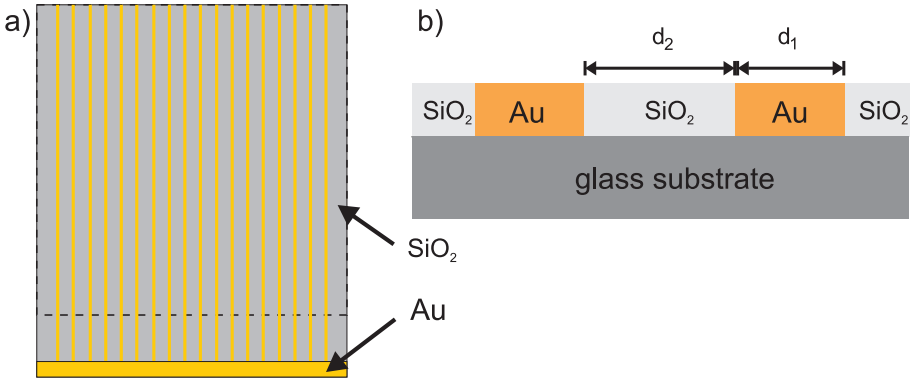

Figure 6. Schematic of the MEMS design. (a) The top view shows the conductive lines embedded in silicon dioxide. (b) The profile shows the thin film on the glass substrate.

The MEMS electrodes differ from the above described electrodes (needle, embedded wire and embedded foil) in the following aspect. The high voltage is not provided from behind, but from the side, and the electrode width $d_1 \geq 10$ μm is greater than its height $d_2 < 1$ μm (the experiments are planned for a variety of combinations of d_1 and d_2). Even though this geometry is very different from the original needle geometry, the principle to produce high electric field strengths where the particles are charged remains the same. We show this with the help of an electrostatic field computation with the finite element method.

The calculation was done for a three-dimensional section of the electrode assembly with a particle lying on the electrode (see Fig. 7). The simulation volume is a cuboid with square base (200 μm$\times$200 μm) which extends from the bottom of the glass substrate to the counter electrode. Due to the undefined boundary conditions at the lateral faces of the simulation volume, the field lines do not cross these faces. This is a good approximation for a periodical continuation in the lateral directions in case of many parallel electrode lines, and even in case of a single electrode line this simplification is justified because of the rapidly decaying potential around the electrode as Fig. 7(a) indicates. An irregular mesh of tetrahedrons was used, which is coarse at the outer boundaries and has high density of vertices at the fine structures.

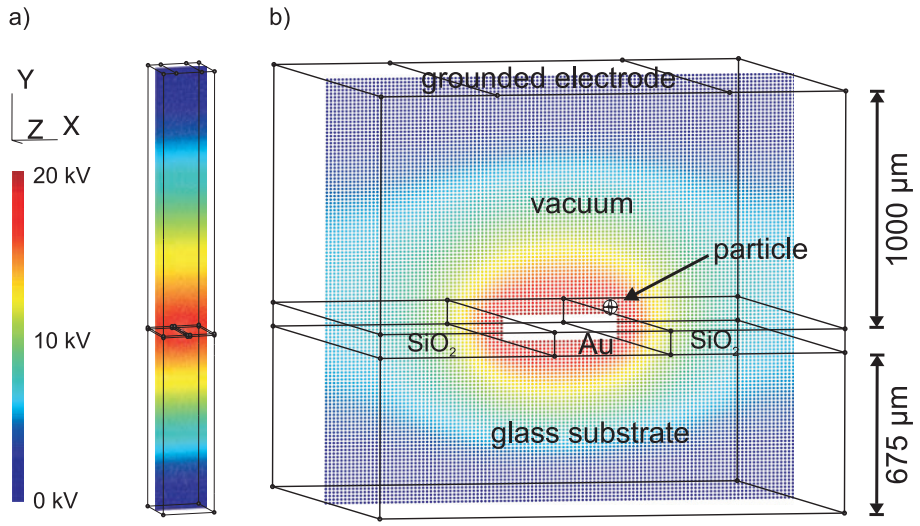

Figure 7. Electrostatic field calculation. (a) The calculated volume is a cuboid with square base (200 μm×200 μm). Line width $d_1 = 10$ μm, particle radius $r_\mathrm{p} = 1.5$ μm. (b) For better visibility of the geometry, the dimensions have been changed in this drawing.

The field solution includes the electric field strengths E_i at the surface elements A_i, from which the surface charge densities $D_i = \epsilon_0 E_i$ can be derived. The particle shown in Fig. 8 has a diameter of $2r_\mathrm{p} = 3$ μm and was charged close to the border of the $d_1 = 10$ μm wide line electrode. Most of the charges are located on the upper hemisphere of the particle yielding a maximum electric field strength of $E_\mathrm{max} = 1.0 \times 10^9$ Vm^{-1}. This value is still an order of magnitude smaller than the critical value for field evaporation. The sum

$$q_\mathrm{p} = \sum_i D_i A_i \tag{5}$$

for all particle's surface elements is the particle charge, in case of the example is $q_\mathrm{p} = 6.6 \times 10^5 e$. An isolated particle with this charge, i.e. after ejection and before its neutralization, would have a surface potential of $\phi_\mathrm{p} = q_\mathrm{p}/(4\pi\epsilon_0 r_\mathrm{p}) \approx +635$ V. Also the electric field force acting on the particle

$$\vec{F} = \sum_i \frac{1}{2} D_i \vec{E}_i \cdot \vec{A}_i \frac{\vec{A}_i}{\|\vec{A}_i\|} \tag{6}$$

can be obtained, which is approximately $F = 18\,\mu$N for the moment of the detachment from the electrode. The kinetic energy the particle gains in the 20 kV acceleration potential is $q_\mathrm{p} U_\mathrm{HV}$ and corresponds to an exhaust velocity of $v_\mathrm{p0} = 445$ m s^{-1} for a gold-coated melamine particle ($\rho = 1510$ kg m^{-3}).

IV. Conclusion

In this paper, we proposed contact charging of solid metal or conductively coated dielectric microparticles and their electrostatic acceleration as a novel thruster concept. Starting from a well known technique applied in experiments for the simulation of micrometeorites,[5,6] improvements with regard to a reliable and high particle charging and a high mass flow rate were proposed and first experiments were presented. Two key features of our improvements are the dielectrical lateral embedding of the fine electrodes and the arrangement of many fine electrodes on a surface. We suggested MEMS as suitable technology and reported on corresponding experiments planned for the near future. Calculations of the expected particle charge and exhaust velocity showed, that speeds of some hundreds of meters per seconds are possible without further acceleration. Higher specific impulses would require an additional downstream acceleration.

Potential applications besides an electrostatic microparticle thruster for space flights are terrestrial utilizations like a refined sand blasting or fast deposition of particles on surfaces. The dielectrically embedded electrodes could also replace the currently used needle particle sources in the dust accelerators for the simulation of micrometeorites.

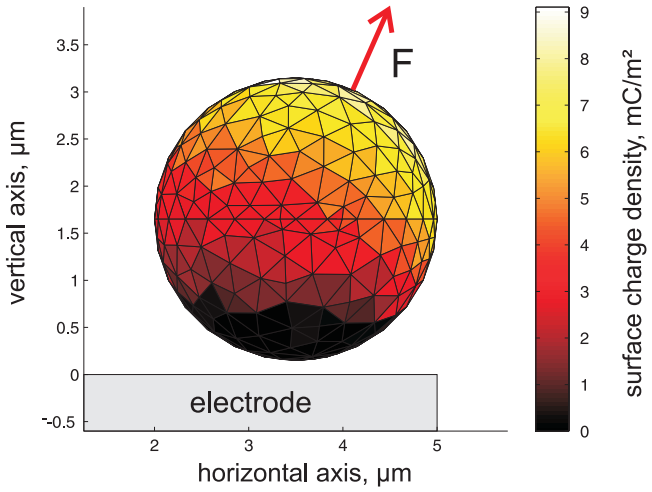

Figure 8. Surface charge density on the particle when it detaches from the electrode. The red arrow indicates the direction of the total force.

Acknowledgments

This work is supported by the German Aerospace Center DLR, Projects No. 50 RS 0802 and No. 50 RS 0902. The technical assistance of Horst Schlüter and Michael Poser is gratefully acknowledged.

References

[1]R. G. Jahn. *Physics of Electric Propulsion.* McGraw-Hill, 1968.

[2]Th. Trottenberg, H. Kersten, and H. Neumann. Feasibility of electrostatic microparticle propulsion. *New J. Phys.* **10**, 063012, 2008.

[3]Paulo Lozano and Manuel Martínez-Sánchez. *Studies on the Ion-Droplet Mixed Regime in Colloid Thrusters.* PhD thesis, MIT, Department of Aeronautics and Astronautics, 2003.

[4]L. Musinski, T. Liu, B. Gilchrist, A. Gallimore, and M. Keidar. Nanoparticle field extraction thruster (nanoFET): Design and results of the microparticle emitter prototype. In *30th International Electric Propulsion Conference, Florence, Italy*, IEPC–2007–80, 2007.

[5]H. Shelton, C. D. Hendricks Jr., and R. F. Wuerker. Electrostatic acceleration of microparticles to hypervelocities. *J. Appl. Phys.* **31**, 1243, 1960.

[6]J. F. Vedder. Charging and acceleration of microparticles. *Rev. Sci. Instr.* **34**, 1175, 1963.

[7]M. Stübig, G. Schäfer, T.-M. Ho, R. Srama, and E. Grün. Laboratory simulation improvements for hypervelocity micrometeorite impacts with a new dust particle source. *Planet. Space Sci.* **49**, 853, 2001.

[8]Erwin W. Müller. Field desorption. *Phys. Rev.* **102**, 618, 1956.

[9]J. Svestka, I. Cermak, and E. Grün. Electric charging and electrostatic fragmentation of dust particles in laboratory. *Adv. Space Res.* **13**, 199, 1993.

[10]J.F. Friichtenicht. Two-million-volt electrostatic accelerator for hypervelocity research. *Rev. Sci. Instrum.* **33**, 209, 1962.